



# Leaching characteristics of naturally derived toxic elements in the alluvial marine clay layer beneath Osaka Plain, Japan: implications for the reuse of excavated soils

Hiroko Ito<sup>1,2</sup> · Harue Masuda<sup>2</sup> · Akihiko Oshima<sup>3</sup>

Received: 18 March 2019 / Accepted: 21 September 2019 / Published online: 4 October 2019  
© Springer-Verlag GmbH Germany, part of Springer Nature 2019

## Abstract

The contamination risks by naturally derived toxic elements must be assessed to achieve a sustainable geo-environment when utilizing excavated surplus soils. To estimate the controlling factors and risks of groundwater pollution associating with the application of recycled excavated surplus soils, the sequentially extracted fractions of major and toxic elements were analyzed and compared to the results of the simple batch leaching test. The concentrations of bulk B and Pb of the Holocene marine clay layer Ma13 were the maximum 75 ppm and 28 ppm at the middle depth and varied similar to the change of clay fraction, while the bulk As concentration was the maximum 12 ppm at the upper part of the Ma13. The B adsorbed onto the clay minerals was easily desorbed under the neutral pH condition. Arsenic was released especially from the transitional sandy silt layers at the upper and lower parts of Ma13 where contacting with oxic groundwater. The 0.45- $\mu\text{m}$  filter required by Japanese regulations does not efficiently remove colloidal particles resulting in poor reproducibility of batch leaching tests, especially for Pb. Also, relative indices of metal mobility suggest that the long-term risk of groundwater contamination via the reuse of excavated surplus soils will not be accurately estimated only by the simple batch leaching test. The change of redox and pH conditions associating with relocation and preservation must be considered to fully evaluate the risk of toxic element mobilization of the excavated surplus soils.

**Keywords** Host phases of toxic elements · Excavated surplus soils · Boron · Arsenic · Lead

**Electronic supplementary material** The online version of this article (<https://doi.org/10.1007/s12665-019-8595-3>) contains supplementary material, which is available to authorized users.

✉ Hiroko Ito  
ito@geor.or.jp

Harue Masuda  
harue@sci.osaka-cu.ac.jp

Akihiko Oshima  
oshima@civil.eng.osaka-cu.ac.jp

<sup>1</sup> Geo-Research Institute, 6F, Kokuminkaikan Sumitomoseimei Bldg. 2-1-2, Otemae, Chuo-ku, Osaka 540-0008, Japan

<sup>2</sup> Department of Biology and Geosciences, Osaka City University, 3-3-138, Sugimoto, Sumiyoshi-ku, Osaka 558-8585, Japan

<sup>3</sup> Department of Urban Design and Engineering, Osaka City University, 3-3-138, Sugimoto, Sumiyoshi-ku, Osaka 558-8585, Japan

## Introduction

Naturally derived toxic elements are a major issue in handling excavated surplus soils in Japan (e.g., Hattori et al. 2007; Okumura et al. 2007; Ito et al. 2013). The toxic trace elements are ubiquitously contained in the soils and underlying sediments irrespective of ore deposits or volcanogenic sediments (e.g., Ito 2012). Under the conventional law, excavated soils with naturally derived toxic element contents exceeding soil environmental standards had to be treated at final waste disposal sites. However, the “Amendment to the Soil Contamination Countermeasures Act” was promulgated in May 2017 (Japanese Ministry of the Environment 2017a) to streamline regulations and promote the effective utilization of naturally derived contaminated soils (Japanese Ministry of the Environment 2017b).

Single-step partial extraction methods enable a rapid evaluation of the level of toxic elements (e.g., Sahuquillo et al. 2003; Alvarez et al. 2011). According to the Japanese law, contaminated areas must be specified based on the analytical

results of simple batch and acid leaching tests based on environmental agency notification nos. 18 and 19 (Japanese Ministry of the Environment 2003a, b, respectively). The similar single-step leaching methods have been developed and used as compliance tests for contaminated soil and waste in many other countries (Yasutaka et al. 2017). These methods were established for the assessments of the health risk to the human body, assuming that soil pollutants are ingested as dissolved matter in groundwater and/or as soil dust. However, the long-term risk of groundwater pollution cannot be evaluated by these analyses, because pollutants in the excavated soil can be mobilized via oxidation when the soil is exposed to aerobic conditions. Thus, various analytical methods have been proposed for more realistic risk assessments of contaminated soils (Public Works Research Institute et al. 2015). Among those, sequential chemical extraction experiments (SCEE) are ones of the critical and widely used techniques that provide the information on the mobilities of toxic elements in soils with changing environmental conditions (e.g., Filgueiras et al. 2002; Hass and Fine 2010; Sutherland 2010). Various SCEE methods have been developed based on Tessier et al. (1979) protocols (e.g., Zimmerman and Weindorf 2010), and the most extensively implemented method is BCR (European Community Bureau of Reference) (Ure et al. 1993) and modified BCR protocols (Rauret et al. 1999). These procedures can forecast the long-term potential level of contamination, although are extremely time consuming; the total time of sample pre-treatment exceeds 50 h (Leśniewska et al. 2016). Kanjo et al. (2008) recommended the modified BCR sequential extraction method to evaluate the long-term contamination risks also in Japan.

Leaching characteristics of naturally derived toxic elements have been studied in several areas in Japan. Cadmium was leached via oxidation–decomposition of cadmium sulfide in the sedimentary rocks in Sendai Plain with lowing pH (Sudo et al. 2010). The concentrations of leached As from the strongly weathered marine sediments were relatively lower than those from the partially oxidized ones under both anaerobic and aerobic conditions (Ogawa et al. 2014). The concentrations of As leached from marine sediments and rocks increased in the solutions with increasing pH > 8.5 because of desorption of As from Fe–oxyhydroxides/oxides (Takahashi et al. 2011; Nishizawa et al. 2012). These studies documented the importance for assessing the leaching properties at changing environmental conditions when excavated surplus soils and rocks are utilized.

The alluvial marine clay layer Ma13 is widely distributed with  $\geq 10$  m thickness beneath the Osaka Plain (KG-NET: Kansai Geo-informatics Network 2007), and contains naturally toxic elements such as As, Pb, F, and B (e.g., Ito et al. 2018). The depth to the top of Ma13 from the ground surface is typically < 10 m (KG-NET: Kansai Geo-informatics

Network 2007), shallower than the maximum investigation depth required by the Japanese law (Japanese Ministry of the Environment 2017c). Thus, it must be an important issue to evaluate the risk of utilizing excavated soils including Ma13. To evaluate Ma13 as a possible pollutant source, its geochemical properties immediately after excavation and the following replacement must be determined. Since most analyses (as required by law) have been performed on soils taken from < 10 m depth, the geochemical and physical characteristics of the entire Ma13 layer have not been studied. Here, bulk sediment chemical analyses, sequential extraction tests, and simple batch leaching tests were performed on cored sediments including Ma13 taken from the western part of the Osaka Plain, and the long-term risk of pollutants via the dissolution of reused soils is evaluated.

## Geological setting of the sampling site

The Osaka Basin (southwest Japan) has been developed since 3 Ma (Ichihara 1993) associating with subduction of Philippine sea plate beneath the Eurasian plate. Osaka Plain occupies the eastern part of this basin, and the Pliocene to Quaternary sediments reach a maximum thickness of 1500 m beneath the plain, and more than 20 marine clay layers (deposited in association with cyclic global sea-level changes) are intercalated with freshwater sand and gravel layers (Ichihara 1993). Holocene sediments, including the uppermost marine clay layer Ma13, widely cover the lowlands of the basin (Fig. 1). The Ma13 exceeds 10 m thickness and thickens toward the western Osaka Bay. In this study, a sediment core from the western Osaka Plain, located on the west of the Uemachi Upland, was analyzed. In this core, the Ma13 was recovered from 6 to 19 m depths from the ground surface (Fig. 2).

## Analytical methods

### Lithology and physical properties of cored sediments

Undisturbed sediments were cored using a thin-walled tube sampler with a diameter of 75 mm (JGS1221-2012; Japanese Geotechnical Society 2015). The sediments were pushed out of the samplers and cut into 10-cm-long cores for laboratory engineering soil tests. For chemical analyses, the 10-cm core segments were vacuum-packed with a de-oxygenizer immediately after cutting to prevent oxidation.

Lithology was described based on visual observation. To identify the depositional ages of the sediments, the refractive indices of the volcanic glass fragments were determined using a refractometer (RIMS, Kyoto

**Fig. 1** Maps of the study site **a** location of the Osaka prefecture, Japan and **b** geological map, distribution area of Ma13 (based on KG-NET: Kansai Geo-informatics Network 2007) and the location of the sampling site (Modified from Ichihara 1993)

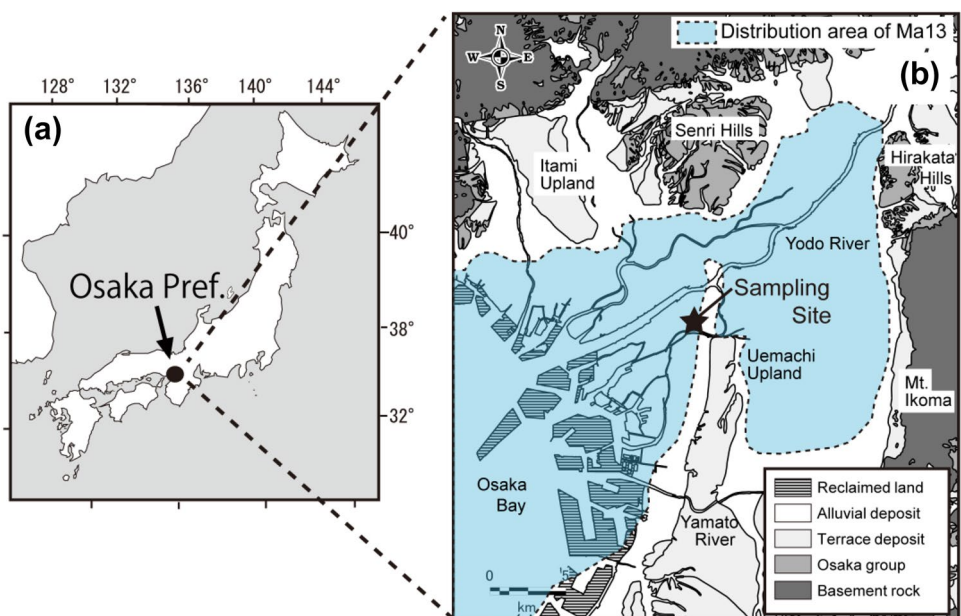
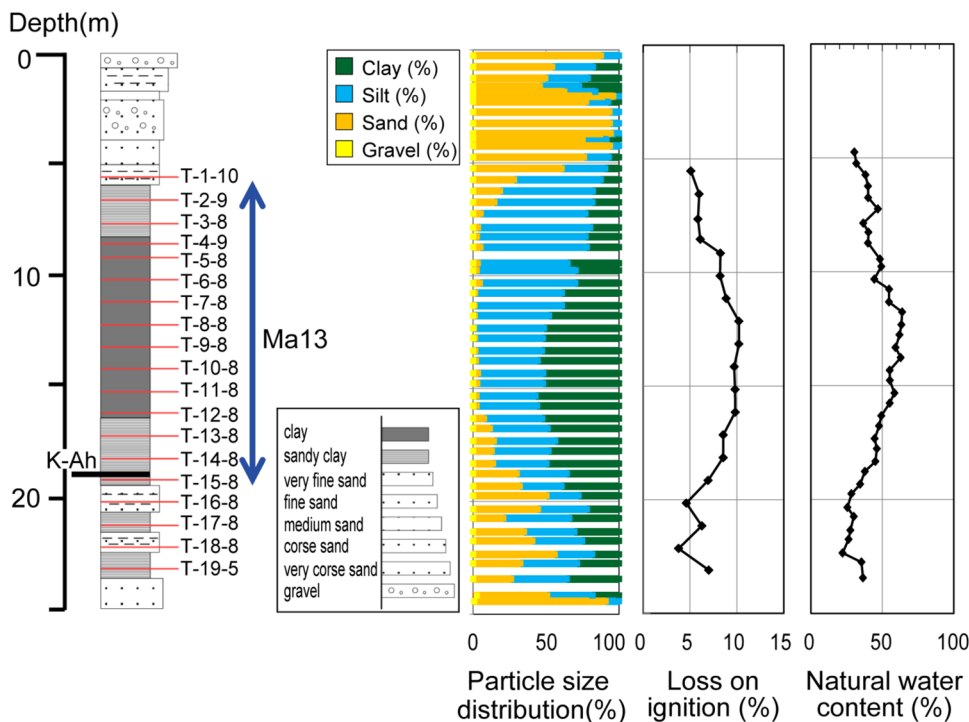


**Fig. 2** Lithology of the studied geologic column with the particle size distribution, loss on ignition, and natural water content



Fission-Track Co., Ltd.) (Danbara et al. 1992) to specify the tephra, depositional age of which was already known. Physical properties of the sediments (i.e., particle size distribution, natural water content, and loss on ignition, LOI) were determined according to Japanese standard methods (JIS A 1204, 1203, and 1226, respectively; Japanese Industrial Standard Association 2009a, b, c).

**Bulk sediment analyses**

The sediment samples stored under anaerobic conditions were freeze-dried and powdered using an agate mortar and pestle. The bulk mineralogy was determined by X-ray powder diffraction (XRD, RAD-1A, Rigaku) with Ni-filtered Cu K $\alpha$  radiation. The samples were also analyzed by XRD

after pretreatment with 1 M HCl to distinguish chlorite and kaolinite, and ethylene glycol to distinguish kaolinite and smectite. Major element concentrations ( $\text{SiO}_2$ ,  $\text{Al}_2\text{O}_3$ ,  $\text{Fe}_2\text{O}_3$ , MnO, MgO, CaO,  $\text{Na}_2\text{O}$ , and  $\text{K}_2\text{O}$ ), were measured by X-ray fluorescence (XRF, VXQ-160S, Shimadzu) using the glass bead method, in which sample powder was fused to make glass bead with lithium borate at maximum temperatures of 1200 °C. The accuracies of major element analyses were within 4% except MnO (within 5%), confirmed by analysis of Geological Survey of Japan (GSJ) geochemical reference sample JB-2. Toxic trace element concentrations (i.e., B, As, Pb, Cr, Cd, and Se) were determined by inductively coupled plasma mass spectrometry (ICP-MS, SPQ9700, SII) using the calibration line method after alkaline fusion of the powdered samples and subsequent dissolution in 0.1 M nitric acid. The accuracies of obtained results were within 10%, confirmed by analyses of GSJ geochemical reference samples JSd-2 and JSd-3.

### Sequential chemical extraction experiment (SCEE)

The freeze-dried samples were sequentially reacted with different chemicals to extract as five fractions: acid-soluble phases, reducible phases, oxidizable phases, insoluble phases, and residual silicates according to the method of Ito et al. (2003), which was modified from that of Thomas et al. (1994) and Wang et al. (1997). This method cannot accurately specify the host phases, but the behaviors of elements with changing environmental redox conditions can be roughly evaluated. The phases were extracted in five steps, as follows.

#### Step 1: acid-soluble phases

One gram of each sediment powder was shaken with 20 mL 0.22 M acetic acid (pH adjusted to five with ammonium acetate) in a PTFE centrifuge tube for 16 h at room temperature. Then the mixture was centrifuged at 10,000 rpm for 10 min to separate the supernatant solution, in which acid-soluble phases were extracted (i.e., components weakly adsorbed onto detrital materials or fixed in carbonates). The supernatant solution was diluted by 0.1 M nitric acid to quantify by ICP-MS.

#### Step 2: reducible phases

The residue from step 1 was shaken with 20 mL 0.5 M hydroxylammonium chloride ( $\text{NH}_3\text{OHCl}$ , pH adjusted to two with  $\text{HNO}_3$ ) for 16 h at room temperature to dissolve reducible phases, mainly Fe-oxyhydroxides and Mn-oxides. Then the mixture was centrifuged at 10,000 rpm for 10 min. The supernatant solution was treated as the same manner as step 1.

#### Step 3: oxidizable phases

The residue from step 2 was heated with 20 mL 0.1 M sodium pyrophosphate for 2 h and then shaken with 10 mL 5 M ammonium acetate ( $\text{CH}_3\text{COONH}_4$ , pH adjusted to two with  $\text{HNO}_3$ ) for 16 h at room temperature. This reagent cannot completely decompose sulfide minerals, so the most probable phase dissolved in this step is organic matter. The mixture was centrifuged at 10,000 rpm for 10 min. Then the supernatant solution was treated as the same manner as step 1.

#### Step 4: insoluble phases

The residue from step 3 was gently heated with a mixture of 10 mL concentrated nitric acid and 8 mL perchloric acid for 24 h, and then shaken for 16 h at room temperature. The mixture was centrifuged at 10,000 rpm for 10 min. The supernatant solution was treated as the same manner as step 1. Most insoluble phases decomposed in this step are silicates and sulfides.

#### Step 5: residual phases (silicates resistant to the above reagents)

The residue from the previous steps was decomposed by alkaline fusion, and the solution was diluted with 0.1 M  $\text{HNO}_3$  to prepare the ICP-MS analysis.

#### Quantification

After extracting at each step, concentrations of major (Na, K, Ca, Mg, Al, Fe, and Mn) and toxic trace elements (B, Cr, As, Pb, Cd, and Se) in the solution were analyzed by ICP-MS as described in “Bulk sediment analyses”. The obtained results were expressed as the weight of leached elements from the powdered sediments (mg/kg, ppm). However, the B, As, and Pb concentrations of leachate after step 1 procedure were directly used for comparison with those of leachate by SBLT (mg/L) described in “Application to effective risk assessments of excavated surplus soils”.

#### Simple batch leaching test (SBLT)

Simple batch leaching test was performed according to Japanese notification no. 46 (Japanese Ministry of the Environment 1991).

Wet sediment samples were air-dried at room temperature for several days and then sieved to remove > 2 mm (gravel) size fraction. Aliquot of the bulk sample 3 g was placed in a 50-mL plastic centrifuge tube with 30 mL water, of which pH was adjusted to 5.8–6.3 with hydrochloric acid and shaken horizontally for 6 h at 200 rpm. The solids were



then collected by centrifugation at 3000 rpm for 20 min, and the supernatant solution was decanted and passed through 0.45- $\mu\text{m}$  and 0.1- $\mu\text{m}$  membrane filters (A045A047A and A010A047A, respectively; Advantec Toyo, Japan). The former filtration procedure was performed according to Japanese notification no. 46, and the latter to evaluate the influence of suspended particles passing through the 0.45- $\mu\text{m}$  filter. In this study, both toxic and major element concentrations in the leached solutions were quantified to estimate the host phases and chemical forms of the toxic elements. Major (Na, K, Ca, Mg, Al, Fe, and Mn) and toxic trace elements (B, Cr, As, Pb, Cd, and Se) in the leachates were measured by ICP-MS as detailed in “Bulk sediment analyses”. Anion concentrations ( $\text{F}^-$ ,  $\text{Cl}^-$ ,  $\text{Br}^-$ , and  $\text{SO}_4^{2-}$ ) in the leached solutions (without added nitric acid) were measured by ion chromatograph (IC1200, Dionex) after filtration with 0.2- $\mu\text{m}$  membrane filter. The obtained results were expressed as the weight of leached elements in the leachates (mg/L) according to Japanese notification no. 46 (Japanese Ministry of the Environment 1991).

## Results

### Lithology

Figure 2 summarizes the lithology and physical properties (particle size distribution, water content, and LOI) of the 19 sediment samples with depth (T-1 to T-19).

Sand fraction was abundant above and below the Ma13, indicating changing depositional conditions during transgressive and regressive sea-level changes associating with Holocene climatic changes. Sediment water content and LOI decreased with increasing sand fraction. Silt and sand fractions were 59–67% and 15–28%, respectively, in the uppermost sediments sampled 5.5–7.0 m depths. The silt fraction ranged 62–77% and the sand fraction decreased to 2.5–5.2% at 7.0–10.4 m depths. Sand pipes and common shells indicated thriving biological activity at 9–10 m depths. These uppermost sedimentary facies suggested a shallow brackish inner bay coastal depositional environment during a regressive period. The middle part of Ma13 (11–16 m depths) comprised silty clay sediments with fragile shell fragments and negligible sand fraction. The most homogeneous clay sediment in the core was observed at 12–13 m depths, suggesting the deepest water depositional environment (i.e., peak sea-level transgression). The maximum paleo-water depth in this study area has not been clarified, though it should be about 15 m below sea-level estimated from the sediment observation near the study site: the water depth at Suminoe (12 km SW of the study area) was 15 m during ca. 6000–5600 cal BP (Yasuhara et al. 2002), and that at Kitatsumori (6 km SW of the study area) was deeper than

15 m during ca. 5500–5000 cal BP (Masuda et al. 2002). Below 16 m depth, sand fraction increased with increasing depth, reaching the maximum > 50% at 20 m and 22 m depths. Based on the theory of sequence stratigraphy (e.g., Vail et al. 1991), these sand-dominated sediments are interpreted as a ravinement surface, i.e., relatively coarse and heterogeneous sediments formed by seafloor erosion during dramatic rises in sea level. Therefore, in this core, typical marine clays were observed at < 20 m depths, and the sediments at 20–23.5 m depths were deposited during large sea-level fluctuations at the beginning of a transgression period.

A concentration of volcanic glass was observed at 19 m depth (just above the ravinement surface) suggesting bioturbation. Volcanic glass particles accounted for 19% of the sediment (among 100 counted sediment grains) at this depth. The refractive indices of these glass fragments indicated that they belonged to the K-Ah (Kikai-Akahoya) tephra, which was originated from Kikai Caldera eruption (Kagoshima prefecture) 7300 years ago and was widely observed in the Japan islands (Machida and Arai 2003). Thus, deposition of Ma13 in seawater of stable depth started around 7000 years ago at this site, consistent with previous results (Masuda et al. 2002).

### Bulk mineralogy and chemistry

XRD analyses revealed the mineralogy of the sediments to be quartz, feldspar, amphibole, pyrite, micas, chlorite, kaolinite, and smectite. XRD intensities of quartz and feldspar (Fig. 3) were positively correlated with sand fraction and negatively correlated with LOI and water content (Fig. 2).  $\text{SiO}_2$  concentrations ranged from 64 to 76 wt% and varied with sand fraction and quartz and feldspar XRD intensities (Fig. 3). These results indicate that the sand fraction mainly comprised quartz and feldspar.

The concentrations of  $\text{Al}_2\text{O}_3$  (12–18 wt%),  $\text{Fe}_2\text{O}_3$  (2.8–6.1 wt%),  $\text{MgO}$  (0.8–2.2 wt%), and  $\text{TiO}_2$  (0.39–0.76 wt%) varied similar to LOI and opposite to  $\text{SiO}_2$  concentration (Figs. 2, 3).  $\text{CaO}$  concentration varied independently from the other major elements, probably due to contamination of biogenic carbonates such as shells and calcareous nanofossils.  $\text{Na}_2\text{O}$  (1.9–2.8 wt%) and  $\text{K}_2\text{O}$  concentrations (2.6–3.0 wt%) slightly decreased and increased with depth, respectively, suggesting an ion-exchange reaction between porewater and clay minerals.

Bulk B (25–75 ppm), Cr (25–75 ppm), and Pb (18–28 ppm) concentrations varied similar to the LOI, water content, and clay fraction (Figs. 2, 3). Bulk As concentrations (5–12 ppm) varied similar to the above three elements, but with the maximum concentration at 9–10 m depths, where the silt fraction was the greatest. Furthermore, the trends of bulk As concentrations with depth were similar to that of  $\text{Fe}_2\text{O}_3$  (Fig. 3), indicating that the As was originated

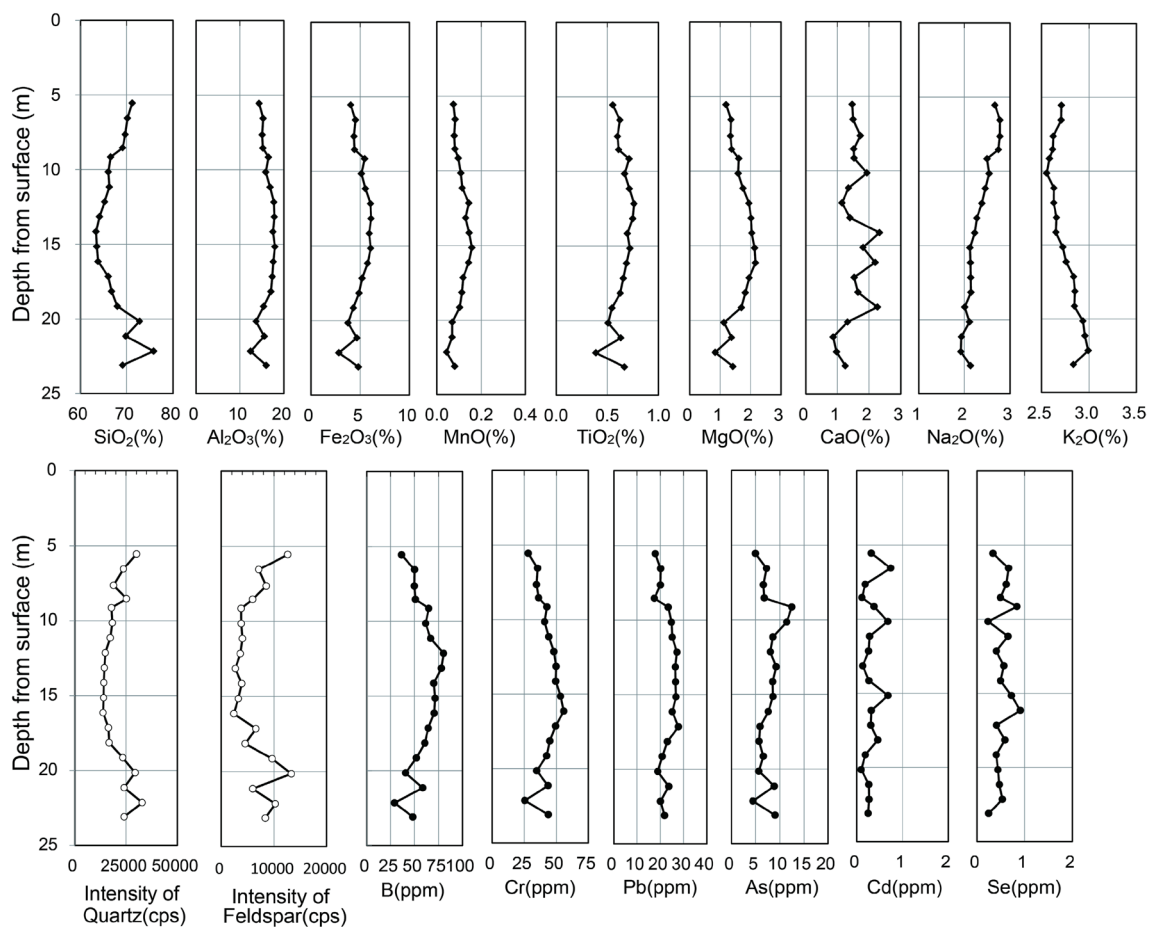


**Fig. 3** Bulk concentrations of major and toxic elements and the XRD intensities of the most intense diffraction peak of quartz ( $d=3.34 \text{ \AA}$ ) and feldspar ( $d=3.19\text{--}3.24 \text{ \AA}$ ) of the sediments from the Osaka Plain, with depth

from iron minerals such as pyrite or Fe-oxyhydroxides/oxides. Bulk Cd and Se contents were  $< 1$  ppm, and it was impossible to observe clear patterns related to the mineralogy or chemical composition of the sediments.

### SCEE

The concentrations of the toxic elements B, As, Pb, and Cr extracted during the SCEE are shown in Fig. 4. The total SCEE concentrations (i.e., the elemental concentrations summed over all extraction steps) accounted for more than 70%, 90%, 80%, and 95% of the bulk B, As, Pb, and Cr concentrations, respectively. Immobile (i.e., insoluble and residual) phases were the most dominant host phases of these four elements.

Boron concentrations in insoluble and residual phases were 11–26 ppm and 4–18 ppm, respectively, with the highest concentrations in the middle of Ma13. The concentration of acid-soluble B (3–15 ppm) was high among the mobile phases, with the highest concentration observed in the middle of Ma13 at 12–13 m depths, where the most

homogeneous clay sediment was observed. B concentrations in acid-soluble and insoluble phases increased with increasing bulk B concentration (Fig. 5a). The acid-soluble B concentration also increased with increasing K and Na concentrations (Fig. 5b). Potassium and Na are easily fixed within clay minerals (e.g., Buatier et al. 1992; Freed and Peacor 1992; Masuda et al. 2001; Iwasaki and Watanabe 1998; Hover and Peacor 1999), and such ion-exchangeable cations are extracted as the acid-soluble phase in this procedure. Therefore, the positive correlations among acid-soluble B, K, and Na (Fig. 5b) imply that the acid-soluble B was desorbed from clay minerals.

Arsenic was most abundant in the insoluble phase (67–87% of the total As extracted, and ranged 3.0–9.4 ppm) with the highest concentration at 9–10 m depths. Insoluble As was strongly and positively correlated with bulk As (Fig. 5c) and positively correlated with insoluble Fe (Fig. 5d), suggesting that the most insoluble As was fixed in sulfide minerals. Oxidizable As concentrations accounted for approximately 8–24% of the total As extracted, and they were higher in the upper part of Ma13 (1.3–2.1 ppm

**Fig. 4** Concentrations of B, As, Pb and Cr extracted by the SCEE of the sediments from Osaka Plain, with depths. See Fig. 2 for the lithology of geological column

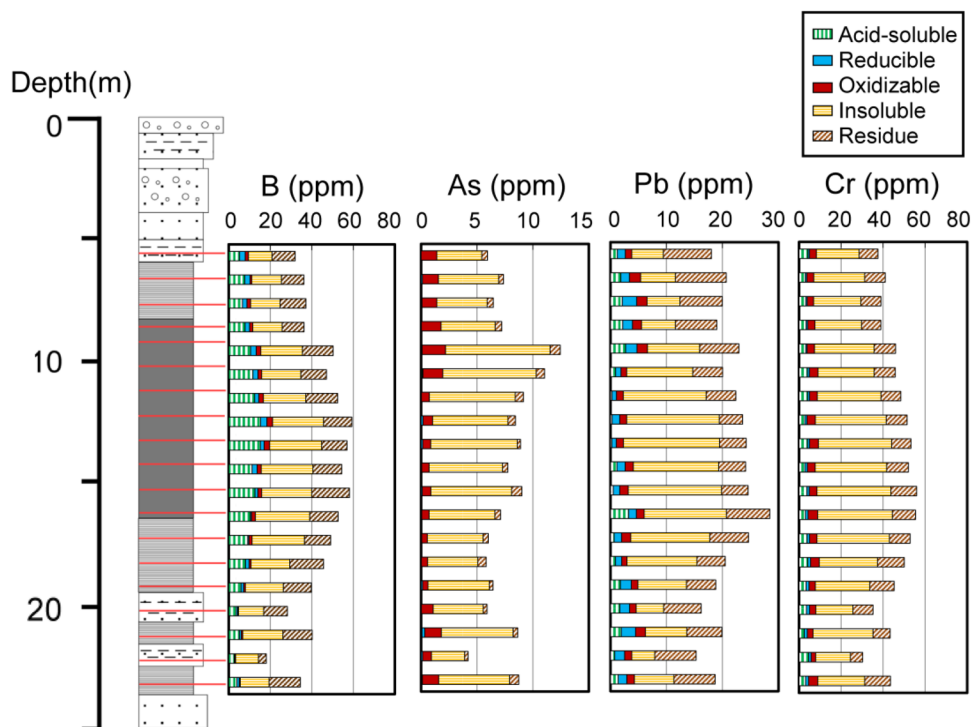
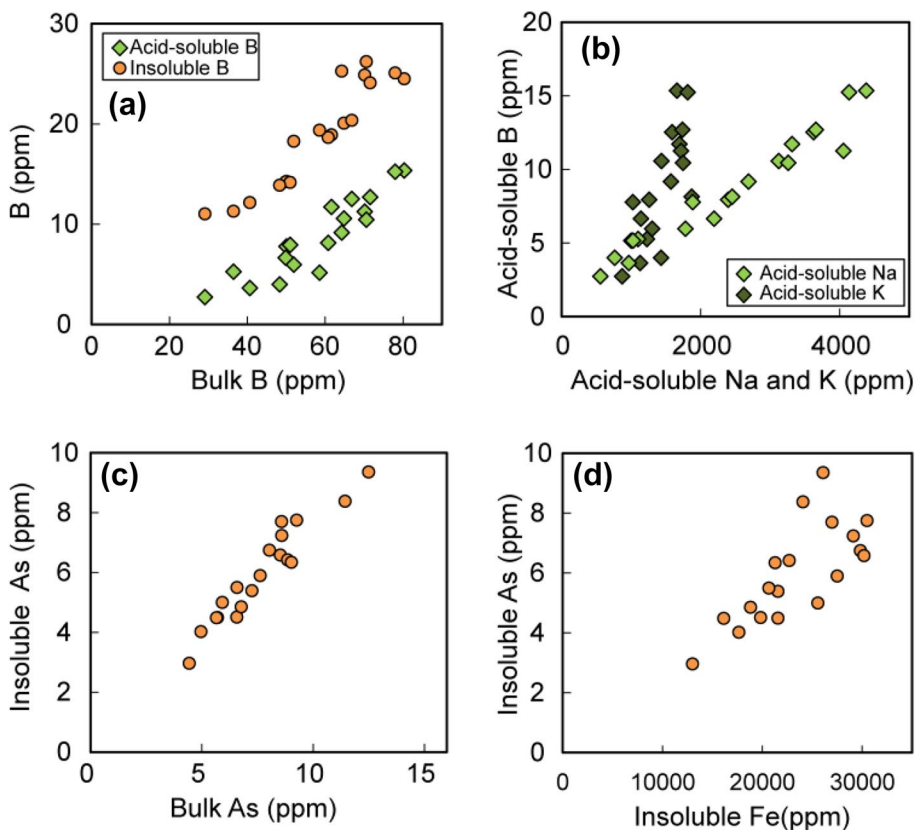


**Fig. 5** Relationships between **a** bulk and acid-soluble and insoluble concentrations of B, **b** acid-soluble concentrations of Na or K and B, **c** bulk and insoluble As concentrations, **d** insoluble Fe and As concentrations



at 5.5–10 m depths) and the sediments underlying Ma13 (1.1–1.5 ppm at 20–21 m and 23 m depths) than in the middle to lower parts of Ma13 (0.7–0.9 ppm at 11–19 m depth). Similar to the maximum insoluble As concentration, the maximum oxidizable As concentration (2.1 ppm) occurred at 9–10 m depths. Acid-soluble and reducible As were negligible compared to the oxidizable and insoluble concentrations.

Immobile Pb accounted for 70–90% of the total Pb extracted. The trend of insoluble Pb was similar to that of bulk Pb, with maximum concentrations at 12–15 m depths. Acid-soluble, reducible, and oxidizable Pb concentrations were higher in the upper and the lowermost parts of Ma13 (5.5–9 m and 19 m depths) and the sediments underlying Ma13 (20–23 m depth) than in the middle to lower parts of Ma13 (10–18 m depths), except at 16 m depth, where the acid-soluble Pb concentration was the highest.

The concentrations of acid-soluble, reducible, and oxidizable Cr were relatively constant with depth, and much lower than the insoluble Cr concentrations, which slightly increased in the middle of Ma13.

## SBLT

Figure 6 shows the results of the SBLT, i.e., the variations of major and toxic element concentrations and pH of leachates in relation to the sampling depth; the analytical results of solutions filtered to 0.1  $\mu\text{m}$  are also compared to those of solutions filtered, per regulation, to 0.45  $\mu\text{m}$  (Fig. 6b, c). The concentrations of Na, K, Ca, Mg, Mn, B, As, Cd, and Se in solutions filtered through the 0.45- $\mu\text{m}$  and 0.1- $\mu\text{m}$  filters are mostly the same, indicating that these elements were mostly dissolved in the solution. On the other hand, the concentrations of Al (0.1–3.1 mg/L), Fe (0.06–0.08 mg/L), Pb (< 0.006 mg/L), and Cr (< 0.007 mg/L) in the 0.45- $\mu\text{m}$ -filtered solutions were higher than those in the 0.1- $\mu\text{m}$ -filtered solutions (Al: < 0.2 mg/L, Fe: 0.01–0.08 mg/L, Cr: 0.002–0.004 mg/L, and Pb: not detected) at 6–9 m, 16 m, and 21–22 m depths. The concentration of Al at 13–14 m depths was also higher in the 0.45- $\mu\text{m}$ -filtered solution.

Na, K,  $\text{Cl}^-$ , and  $\text{Br}^-$  concentrations produced arcuate trends with the lowest concentrations at the top and bottom of the studied section, and maximum concentrations at 12–13 m depths, in the middle of Ma13 (Fig. 6a, b). The  $\text{Cl}^-$  and  $\text{Br}^-$  concentrations were strongly and positively correlated (Fig. 7a). These halogens originate in seawater, and indeed, their maximum concentrations were observed in the deepest water interglacial sedimentation facies. Na and K concentrations were above typical seawater values (Fig. 7b, c), suggesting that they were added by mineral dissolution and/or ion-exchange reactions with clay minerals during the leaching test. The trends of K and Mg concentrations with

depth were similar to that of  $\text{SO}_4^{2-}$  (i.e., having multiple maxima within Ma13). pH values were between 7.0 and 7.5, but decreased to 5.2 in the lowermost sediment analyzed.

$\text{F}^-$  concentrations throughout Ma13 (up to 1.5 mg/L) exceeded the upper limit of Japanese regulations (0.8 mg/L), whereas other toxic elements were below regulation limits except for two samples: As at 9 m depth (regulation value 0.01 mg/L) and B at 11–12 m depths (0.1 mg/L). The maximum B concentration (12 m depth) occurred where the  $\text{Cl}^-$  concentration was the highest (290 ppm), and the B/ $\text{Cl}^-$  ratios were well above the seawater–freshwater mixing line (SW in Fig. 7d). Pb was only detected in the 0.45- $\mu\text{m}$ -filtered solutions at 6–9 m, 16 m, and 21–22 m depths (maximum 0.006 mg/L at 9 m depth). The maximum bulk Cr concentration was lower than the regulation value (0.01 mg/L as hexavalent ion). Arsenic concentrations were high at 6–9 m and 16–19 m depths of the Ma13 deposited during regression and transgression periods, respectively. Cd concentrations were very close to the detection limit (0.05  $\mu\text{g/L}$ ). Se concentrations were generally low (< 0.002 mg/L), but slightly high at the uppermost parts of Ma13.

## Discussion

### Factors controlling the dissolved concentrations of toxic elements

As noted above, the groundwater pollution risk by excavated surplus soils is legally evaluated based on the water-soluble fractions extracted by the SBLT. However, because this test does not account for the redox-dependent mobilities of toxic elements in the environment, it is important to specify the host phases and factors controlling the solubilities of naturally derived toxic elements for utilizations of naturally contaminated excavated surplus soils. Here, the factors controlling the mobilities of B, As, and Pb are discussed.

In the SBLT, about 10% of the bulk B was water soluble. The SCEE indicated that B was mainly hosted in acid-soluble and insoluble phases, which occur in relatively high proportions in clay-rich sediments. B is adsorbed predominantly on clay minerals (Williams et al. 2001), and strong positive correlations are observed between clay fractions and adsorbed B concentrations (Goldberg and Glaubig 1986). Water-soluble B concentrations were clearly high in the studied sediments with high proportions of silt and smaller size fractions (Figs. 2, 3, 6). The highest water-soluble B concentration was observed at 12–13 m depths, where the highest  $\text{Cl}^-$ ,  $\text{Br}^-$ , Na, and K concentrations were observed. Thus, this highly mobile B is likely derived from seawater, in which the B concentration is typically 4.5 ppm, 450 times higher than the average value



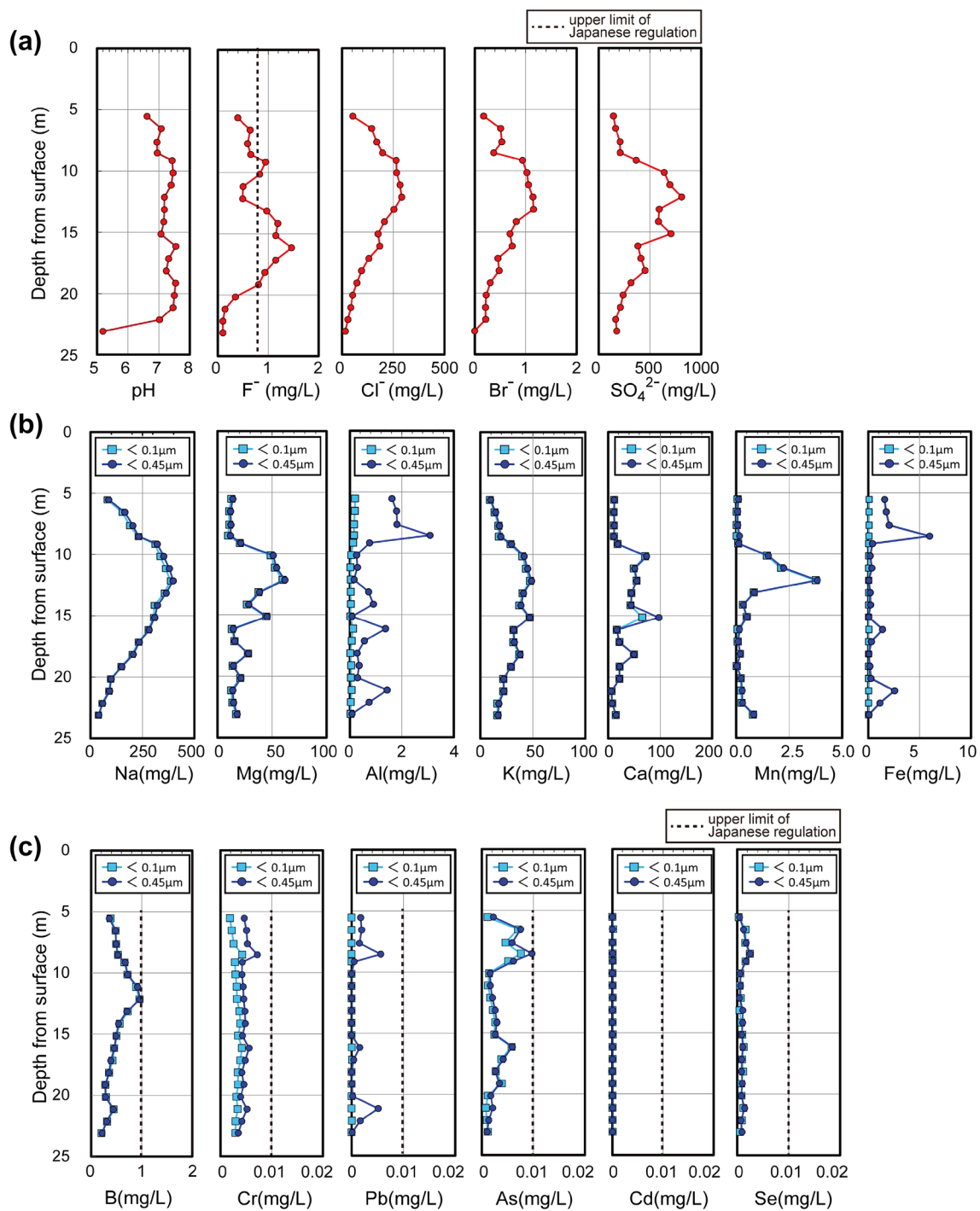


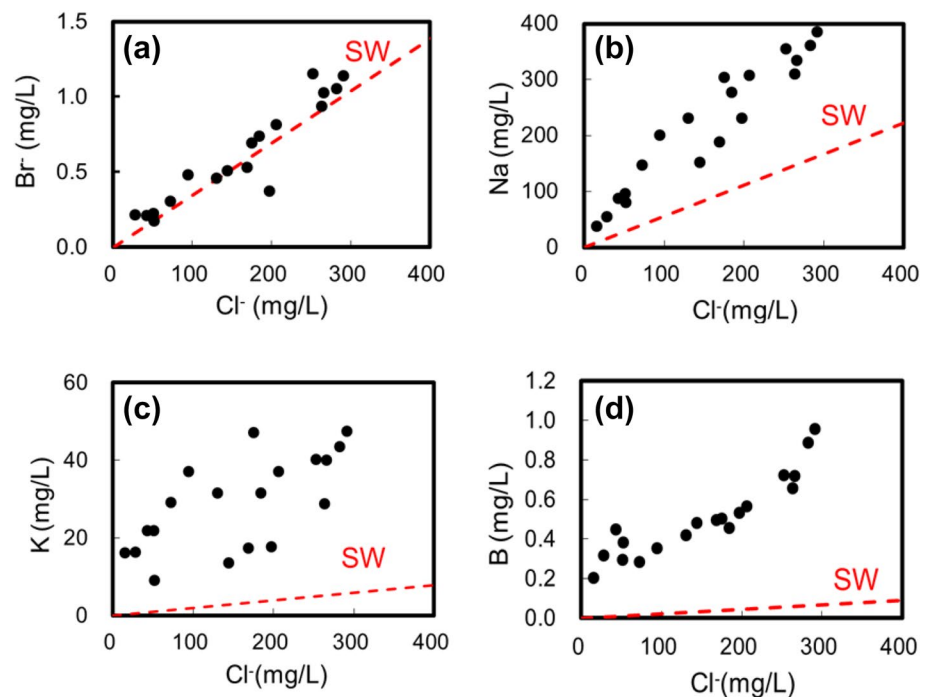
**Fig. 6** Concentrations of chemical components in the leachates treated by the SBLT. **a** pH and anion concentrations of <0.2-μm-filtered solutions, **b** major cation concentrations of <0.45

and <0.1-μm-filtered solutions, **c** toxic trace element concentrations of <0.45 and <0.1-μm-filtered solutions (Recompiled from Ito et al. (2018))

of stream waters (Faure 1998). In the studied sediments, B was adsorbed onto clay minerals such as chlorite, kaolinite, smectite, and micas (as detected by XRD analysis). Adsorbed B is easily desorbed from clay particles under the pH conditions of the SBLT solutions (mostly 7.0–7.5).

At such pH conditions, B exists as the neutral oxyhydroxide B(OH)<sub>3</sub> (Choi and Chen 1979), which is incorporated along with water molecules in the interlayer of expandable smectite minerals (Williams and Hervig 2005; Williams et al. 2007; Osawa et al. 2010). Thus, in the SBLT,

**Fig. 7** Relationships of concentrations between  $\text{Cl}^-$  and **a**  $\text{Br}^-$ , **b** Na, **c** K and **d** B. SW gives the seawater–freshwater mixing line



B would be extracted as an acid-soluble phase along with other ion-exchangeable cations such as Na and K (Fig. 5b).

Bulk As concentrations were within the ranges reported for global present-day marine clays (3–15 ppm, Smedley and Kinniburgh 2002), in seabed sediments of Osaka Bay (e.g., 3–15 ppm,  $n=9$ , Geological Survey of Japan (AIST) 2018; 5–13 ppm,  $n=15$ , Osaka Prefecture Government 2018), and in Ma13 (6–26 ppm, Mitamura and Masuda 1998). The As of this study was mostly present as oxidizable and insoluble phases. Among the insoluble phases, sulfide minerals are important sources of As. The primary As-bearing sulfides are formed in association with magmatism and related hydrothermal activities (e.g., Matschullat 2000; Masuda 2018), though diagenetic sulfide minerals can also be important sources of As. In particular, pyrite commonly found in sedimentary formations contains > 2% As (e.g., Savage et al. 2000; Akai et al. 2004). Since the studied sediments contained pyrite at a level detectable by XRD analysis (i.e., on the order of a percent), a considerable amount of As must be incorporated into pyrite during diagenesis.

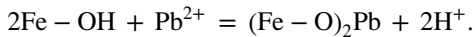
The maximum concentration of insoluble As was observed at 9–10 m depths, consistent with the trend of bulk As. Estuarine sediments from the southwestern Osaka Plain (Suminoe region), similar to our sediments at 9–10 m depths, were plausibly deposited at < 10 m water depth (Yasuhara et al. 2002), where benthic organisms have high production volumes (Nixon 1988; Yamaguchi and Montani 2002). The concentrations of oxidizable (organic) As were also relatively high in the sediments at the same depth, implying As accumulation by marine biological processes

since marine plants and algae easily accumulate inorganic As from seawater and partly transform it into organic forms (Francesconi and Edmonds 1996; Neff 2002). Biologically promoted reducing environments occur in sediments associated with the decomposition of organic matter. Authigenic framboidal pyrite is commonly formed at ambient temperatures closely associated with activity of sulfate reducing bacteria (e.g., Kohn et al. 1998; Popa et al. 2004; Mozer 2010). Although it is difficult to fully explain the relationship of As and sulfide minerals observed herein, the insoluble As may have been partially fixed in authigenic pyrite under a biologically promoted reducing environment, especially at 9–10 m depths in the core.

Water-soluble As concentrations extracted by the SBLT were relatively high in the sediments at 6–9 m and 16–19 m depths. Those sediments were sandy silts with shells and bioturbations, suggesting their deposition in a shallow inner bay environment during regression and transgression periods. The sand fraction gradually decreased from 19 to 3% and increased from 3 to 30% with increasing depth in the 6–9 m and 16–19 m depth intervals, respectively. These sandy silt sediments are the uppermost and lowermost sediments of Ma13, contacting with adjacent coarse sediment layers that act as groundwater aquifers. Therefore, As continuously released via oxidation–decomposition reactions of oxidizable and/or insoluble As phases in flowing groundwaters must have been adsorbed onto clay particles and/or other mineral surfaces.

The concentrations of water-soluble Pb in the 0.45- $\mu\text{m}$ -filtered solutions were clearly higher than those in

the 0.1- $\mu\text{m}$ -filtered solutions and had the similar trends to those of Al and Fe (i.e., generally low concentrations with a prominent peak, Fig. 6), suggesting that colloidal particles passed through the 0.45- $\mu\text{m}$  filter with the adsorbed Pb. Fe- and Al-hydroxides are known to combine with metal ions as surface complexes. For example,  $\text{Pb}^{2+}$  can be adsorbed onto the Fe-hydroxide surface by the following reaction (Wada 2008):



The ability of  $\text{Pb}^{2+}$  to bond to Fe- and/or Al-hydroxides decreases with decreasing pH (McGarvey et al. 1999). Thus, the  $\text{Pb}^{2+}$  was dissolved from surface complexes in the diluted nitric acid solution prepared for ICP-MS analyses. Importantly, these results confirm previous reports that the 0.45- $\mu\text{m}$  filter is not sufficient to completely remove suspended particles, which affects evaluations of the mobility of certain toxic elements such as Pb (e.g., Yasutaka et al. 2017; Imoto et al. 2018; Ito et al. 2018).

### Application to effective risk assessments of excavated surplus soils

For effective and realistic risk assessments of the reuse of excavated surplus soils, the relative index of metal mobility (mobility factor, MF) has been defined as the ratio of the sum of water-extractable, ion-exchangeable, and acid-soluble metal concentrations to the bulk metal concentration (e.g., Kabala and Singh 2001; Kanjo et al. 2008). Here, because toxic elements in water-extractable and ion-exchangeable phases were extracted as acid-soluble phases in step 1 of the SCEE, the ratios of toxic element concentrations in acid-soluble phases to their bulk concentrations are regarded as MFs. The calculated MFs were 12–27% for B, < 0.8% for As, and 1–12% for Pb. These values were also expressed as concentrations in the acid-soluble leaching solutions (mg/L), which reacted under the same ratio of liquid (L) (mL) to sediment (S) (g) as SBLT ( $L/S = 10$ ), for comparison with water-soluble concentrations (Fig. 8). The acid-soluble concentrations of B, As, and Pb were 0.27–1.54, < 0.008, and 0.02–0.32 mg/L, respectively, i.e., 2.6, 7, and > 40 times larger than their respective water-soluble concentrations (Fig. 8). These results suggest that the long-term risk of groundwater contamination from the reuse of excavated surplus soils is underestimated by the regulation (0.45- $\mu\text{m}$  filter) SBLT. For Pb specifically, the maximum recalculated concentration in the leaching solutions (0.32 mg/L) is 32 times larger than the regulatory limit (0.01 mg/L), although the concentrations of water-soluble Pb were negligible when colloidal particles were filtered out (0.1- $\mu\text{m}$  filter).

Leaching of B, As, and Pb from the analyzed marine clay sediments must be accelerated in oxic aqueous environments. For example, As dissolution accompanies the

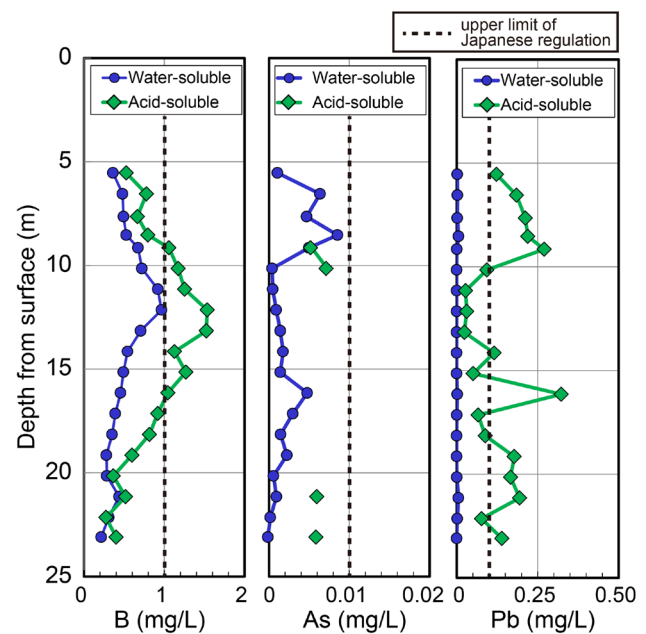
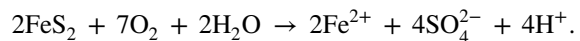


**Fig. 8** Comparisons of concentrations of B, As, and Pb leached into water-soluble and acid-soluble fractions from the sediments reacted under the same liquid to sediment ratio with depth. The ratio (L/S) was 10 mL/g

oxidation of pyrite with decreasing pH by the following reaction:



This reaction can also accelerate the leaching of B and Pb from sediments. This reaction is one of the most realistic mechanisms for multiple toxic-element groundwater pollution resulting from the reuse of marine sediment-derived excavated surplus soils.

### Conclusions

Holocene marine clay sediments in shallow coastal basins represent a contamination risk when exposed to environmental conditions differing from their in situ underground conditions. Thus, excavated soils containing such clay sediments must be carefully treated when reused. In many cases, leaching of toxic elements from the soils would be accelerated by in situ oxidation reactions. Therefore, excavated soils should be stored in reducing conditions, although they are generally exposed to aerobic conditions when reused in construction sites. For risk assessments of groundwater pollution resulting from the reuse of excavated soils, it is best to analyze soils more rigorously than required by regulations. Furthermore, it is necessary to continuously monitor any impacts on the surrounding environment after the reuse of excavated soils. From the point of views of reducing construction waste

to achieve a sustainable geo-environment, our methods are more appropriate than those currently required to evaluate the risks of reusing extracted surplus soils, especially when considering long-term effects.

**Acknowledgements** The authors thank N. Kitada and T. Fujiwara for sampling, and K. Okazaki for analytical assistance in the laboratory.

## References

- Akai J, Izumi K, Fukuhara H, Masuda H, Nakano H, Yoshimura T, Ohfuji H, Md Anwar H, Akai K (2004) Mineralogical and geomicrobiological investigations on groundwater arsenic enrichment in Bangladesh. *Appl Geochem* 19:215–230
- Alvarez MB, Domini CE, Garrido M, Lista AG, Fernández-Band BS (2011) Single-step chemical extraction procedures and chemometrics for assessment of heavy metal behaviour in sediment samples from the Bahía Blanca estuary, Argentina. *J Soils Sediments* 11:657–666
- Buatier MD, Peacor DR, O’Neil JR (1992) Smectite-illite transition in Barbados accretionary wedge sediments: TEM and AEM evidence for dissolution/crystallization at low temperature. *Clay Clay Miner* 40:65–80
- Choi W-W, Chen KY (1979) Evaluation of boron removal by adsorption on solids. *Environ Sci Technol* 13:189–196
- Danhara T, Yamashita T, Iwano H, Kasuya M (1992) An improved system for measuring reflective index using the thermal immersion method. *Quatern Int* 13(14):89–91
- Faure G (1998) Principles and applications of geochemistry, 2nd edn. Prentice Hall in Upper Saddle River, New Jersey
- Filgueiras AV, Lavilla I, Bendicho C (2002) Chemical sequential extraction for metal partitioning in environmental solid samples. *J Environ Monit* 4:823–857
- Francesconi KA, Edmonds JS (1996) Arsenic and marine organisms. *Adv Inorg Chem* 44:147–189
- Freed RL, Peacor DR (1992) Diagenesis and the formation of authigenic illite-rich I/S crystals in gulf coast shales: TEM study of clay separates. *J Sediment Petrol* 62:220–234
- Geological Survey of Japan (AIST) (2018) Geochemical map of sea and land of Japan. <https://gbank.gsj.jp/geochemmap/ocean/data/seadata.htm>. Accessed 18 Dec 2018 (in Japanese)
- Goldberg S, Glaubig RA (1986) Boron adsorption on California soils. *Soil Sci Soc Am J* 50:1173–11176
- Hass A, Fine P (2010) Sequential selective extraction procedures for the study of heavy metals in soils, sediments, and waste materials: a critical review. *Environ Sci Technol* 40:365–399
- Hattori S, Ohta T, Kikuchi Y (2007) Assessment of judgment standard for acid water drainage from rock muck at the Hakkouda tunnel. *J Jpn Soc Eng Geol* 47(6):323–336 (in Japanese with English abstract)
- Hover VC, Peacor DR (1999) Direct evidence for potassium uptake in smectite during early diagenesis of marine sediments and MORB: balancing the global potassium budget. Clay mineral society meeting program and abstracts, 36th Annual Meeting, Purdue University, West Lafayette, p 50
- Ichihara M (ed) (1993) The Osaka Group. Sogen-sha, Osaka. ISBN 4422220039 (in Japanese)
- Imoto Y, Yasutaka T, Someya M, Higashino K (2018) Influence of solid-liquid separation method parameters employed in soil leaching tests on apparent metal concentration. *Sci Total Environ* 624:96–105
- Ito K (2012) Soil, clay and minerals on metals contaminated groundwater and soil. *Nendokagaku (J Clay Sci Soc Jpn)* 50(3):144–153 (in Japanese with English abstract)
- Ito H, Masuda H, Kusakabe M (2003) Some factors controlling arsenic concentrations of groundwater in the northern part of Osaka prefecture. *J Groundw Hydrol* 45(1):3–18 (in Japanese with English abstract)
- Ito T, Ito S, Nagata H (2013) Management system on the tunnel goaf with natural heavy metal. *J Jpn Soc Civil Eng Ser F4* 69(4):I\_137–I\_144 (in Japanese with English abstract)
- Ito H, Masuda H, Oshima A (2018) Concentrations of the naturally-derived toxic elements and its geochemical characteristics of the alluvial marine clay layer of Osaka Plain, Japan. In: Proceedings of the 8th International Congress on Environmental Geotechnics, vol 1, pp 504–511
- Iwasaki T, Watanabe T (1998) Distribution of Ca and Na ions in dioctahedral smectites and interstratified dioctahedral mica/smectites. *Clay Clay Miner* 36(1):73–82
- Japanese Geotechnical Society (2015) JGS 1221–2012 method for obtaining soil samples using thin-walled tube sampler with fixed piston. Japanese geotechnical society standards: geotechnical and geo-environmental investigation methods, 1st edn. Maruzen Publishing Co., Ltd., Tokyo. ISBN 978-4-88644-820-0
- Japanese Industrial Standard Association (2009a) JIS A 1204 test method for particle size distribution of soils. <http://www.jisc.go.jp/app/jis/general/GnrJISSearch.html>. Accessed 4 Jan 2019 (in Japanese)
- Japanese Industrial Standard Association (2009b) JIS A 1203 test method for water content of soils. <http://www.jisc.go.jp/app/jis/general/GnrJISSearch.html>. Accessed 4 Jan 2019 (in Japanese)
- Japanese Industrial Standard Association (2009c) JIS A 1226 test method for ignition loss of soils. <http://www.jisc.go.jp/app/jis/general/GnrJISSearch.html>. Accessed 4 Jan 2019 (in Japanese)
- Japanese Ministry of the Environment (1991) Environmental agency notifications no. 46 (environmental standards relating to contamination of soil). <http://www.env.go.jp/kijun/dojou.html>. Accessed 25 Feb 2019 (in Japanese)
- Japanese Ministry of the Environment (2003a) Environmental agency notifications no. 18 (analytical methods of simple batch leaching test). <https://www.env.go.jp/water/dojo/law/kokuji.html>. Accessed 25 Feb 2019 (in Japanese)
- Japanese Ministry of the Environment (2003b) Environmental agency notifications no. 19 (analytical methods of acid leaching test). <https://www.env.go.jp/water/dojo/law/kokuji.html>. Accessed 25 Feb 2019 (in Japanese)
- Japanese Ministry of the Environment (2017a) Amendment to the soil contamination countermeasures act. [http://elaws.e-gov.go.jp/search/elawsSearch/elaws\\_search/lsg0500/detail?lawId=414AC0000000053](http://elaws.e-gov.go.jp/search/elawsSearch/elaws_search/lsg0500/detail?lawId=414AC0000000053). Accessed 25 Feb 2019 (in Japanese)
- Japanese Ministry of the Environment (2017b) Enforcement notice of the soil contamination countermeasures act, no. 1703313. [https://www.env.go.jp/water/dojo/law/kaisei2009/no\\_100305002.pdf](https://www.env.go.jp/water/dojo/law/kaisei2009/no_100305002.pdf). Accessed 25 Feb 2019 (in Japanese)
- Japanese Ministry of the Environment (2017c) Enforcement regulation of the soil contamination countermeasures act, ordinance no. 29 of ministry of the environment. [http://elaws.e-gov.go.jp/search/elawsSearch/elaws\\_search/lsg0500/detail?lawId=414M60001000029](http://elaws.e-gov.go.jp/search/elawsSearch/elaws_search/lsg0500/detail?lawId=414M60001000029). Accessed 25 Feb 2019 (in Japanese)
- Kabala C, Singh BR (2001) Fractionation and mobility of copper, lead, zinc in soil profiles in the vicinity of a copper smelter. *J Environ Qual* 30:485–492
- Kanjo Y, Nouri M, Kase T (2008) Application of modified BCR sequential extraction procedure for evaluation of heavy metal leaching in contaminated soil. *J Jpn Soc Civil Eng G64(4):304–313 (in Japanese with English abstract)*



- Kansai Geo-informatics Network (KG-NET) (2007) Shi-Kansai Jiban-from Osaka Plain to Osaka Bay area. KG-NET (**in Japanese**)
- Kohn MJ, Riciputi LR, Stakes D, Orange DL (1998) Sulfur isotope variability in biogenic pyrite: reflections of heterogenous bacterial colonization? *Am Miner* 83:1454–1468
- Leśniewska B, Kisielewska K, Wiater J, Godlewska-Żyłkiewicz B (2016) Fast and simple procedure for fractionation of zinc in soil using an ultrasound probe and FAAS detection. Validation of the analytical method and evaluation of the uncertainty budget. *Environ Monit Assess* 188:29. <https://doi.org/10.1007/s10661-015-5020-6>
- Machida H, Arai F (2003) Atlas of tephra in and around Japan. University of Tokyo Press, Tokyo (**in Japanese**). ISBN 4-13-060745-6
- Masuda H (2018) Arsenic cycling in the earth's crust and hydrosphere: interaction between naturally occurring arsenic and human activities. *Prog Earth Planet Sci* 5:68
- Masuda H, Peacor DR, Dong H (2001) Transmission electron microscopy study of conversion of smectite to illite in mudstones of the Nankai trough: contrast with coeval bentonites. *Clay Clay Miner* 49(2):109–118
- Masuda F, Irizuki T, Fujiwara O, Miyahara B, Yoshikawa S (2002) A Holocene sea-level curve constructed from a single core at Osaka, Japan (a preliminary note). *Ser Geol Miner* 59(1):1–8
- Matschullat J (2000) Arsenic in geosphere: a review. *Sci Total Environ* 249:297–312
- McCarvey GB, Ross KJ, McDougall TE, Turner CW (1999) Lead corrosion and transport in simulated secondary feedwater. Atomic energy of Canada limited. [https://inis.iaea.org/Collection/NCLCollectionStore/\\_Public/31/030/31030413.pdf](https://inis.iaea.org/Collection/NCLCollectionStore/_Public/31/030/31030413.pdf). Accessed 9 Jan 2019 (ISSN 0067-0367)
- Mitamura M, Masuda H (1998) Arsenic content of drilling cores in Osaka and its surrounding area. In: Proceedings of the 8th Symposium on Geo-Environments and Geo-Technics, pp 85–88 (**in Japanese with English abstract**)
- Mozer A (2010) Authigenic pyrite framboids in sedimentary facies of the Mount Wavel formation (eocene), King George Island, west Antarctica. *Pol Polar Res* 31(3):255–272
- Neff JM (2002) Chapter 3: arsenic in the ocean. In: Bioaccumulation in marine organisms: effect of contaminants from oil well produced water. Elsevier Science, pp 57–78. ISBN 9780080527840
- Nishizawa T, Kato M, Kitazawa H, Sato T (2012) Chemical speciation and release of arsenic to groundwater in Seino Basins, Nobi Plain. *J Jpn Soc Civil Eng Ser C* 68(4):670–679 (**in Japanese with English abstract**)
- Nixon SW (1988) Physical energy inputs and the comparative ecology of lake and marine ecosystems. *Limnol Oceanogr* 33:1005–1025
- Ogawa Y, Masuda S, Shinoda K (2014) Arsenic dissolution from waste dumps containing marine sediment. *J Geogr* 123(6):936–948 (**in Japanese with English abstract**)
- Okumura K, Sakurai K, Nakamura N, Morimoto Y (2007) Environmental impacts of naturally-occurring heavy metals and countermeasures. *J Geogr* 116(6):892–905 (**in Japanese with English abstract**)
- Osaka Prefecture Government (2018) Results of sea bottom sediments investigation in Osaka Bay, 2012. <http://www.pref.osaka.lg.jp/kankyohozen/osaka-wan/teisitsu.html>. Accessed 18 Dec 2018 (**in Japanese**)
- Osawa S, Amita M, Yamada M, Mishima T, Kazahaya K (2010) Geochemical features and genetic process of hot-spring waters discharged from deep hot-spring wells in the Miyazaki Plain, Kyushu island, Japan: diagenetic dehydrated fluid as a source fluid of hot-spring water. *J Hot Spring Sci* 59:295–319 (**in Japanese with English abstract**)
- Popa R, Kinkle BK, Badescu A (2004) Pyrite framboids as biomarkers for iron-sulfur systems. *Geomicrobiol J* 21:193–206
- Public Works Research Institute et al (2015) Handbook of excavated surplus soils containing naturally-derived heavy metals. Taisei Shuppan, Tokyo (**in Japanese**). ISBN 978-4-8028-3193-2
- Rauret G, López-Sánchez JF, Sahuquillo A, Rubio R, Davidson C, Ure A, Quevauvillerc P (1999) Improvement of the BCR three step sequential extraction procedure prior to the certification of new sediment and soil reference materials. *J Environ Monit* 1(1):57–61
- Sahuquillo A, Rigol A, Rauret G (2003) Overview of the use of leaching/extraction tests for risk assessment of trace metals in contaminated soils and sediments. *Trends Anal Chem* 22:152–159
- Savage KS, Tingle TN, O'Day PA, Waychunas GA, Bird DK (2000) Arsenic speciation in pyrite and secondary weathering phases, Mother Lode gold district, Tuolumne County, California. *Appl Geochem* 15:1219–1244
- Smedley PL, Kinniburgh DG (2002) A review of the source, behavior and distribution of arsenic in natural waters. *Appl Geochem* 17:517–568
- Sudo K, Yoneda T, Ogawa Y, Yamada R, Inoue C, Tsuchiya N (2010) Effect of weathering on changes of leaching properties and chemical forms of heavy metals in a sedimentary rock of Tatsunokuchi formation. *J Jpn Soc Eng Geol* 51(4):181–190 (**in Japanese with English abstract**)
- Sutherland RA (2010) BCR<sup>®</sup>-701: a review of 10 years of sequential extraction analyses. *Anal Chim Acta* 680(1–2):10–20
- Takahashi R, Kakihara Y, Hara J, Komai T (2011) Leaching process of arsenic from sedimentary rocks and change in leaching amount with weathering: examples from the Miocene Kawabata and Karumai formations, central Hokkaido, Japan. *J Geol Soc Jpn* 117(10):565–578 (**in Japanese with English abstract**)
- Tessier A, Campbell PGC, Bisson M (1979) Sequential extraction procedure for the speciation of particulate trace metals. *Anal Chem* 51(7):844–851
- Thomas RP, Ure AM, Davison CM, Littlejohn D, Rauret G, Rubio R, Lopez-Sanches JF (1994) Three-stage sequential extraction procedure for the determination of metals in river sediments. *Anal Chem Acta* 286:423–429
- Ure AM, Quevauviller P, Muntau H, Griepink B (1993) Speciation of heavy metals in soils and sediments. An account of the improvement and harmonization of extraction techniques undertaken under the auspices of the BCR of the Commission of the European Communities. *Int J Environ Anal Chem* 51:135–151
- Vail PR, Audemard F, Boeman SA, Eisner PN, Perez-Cruz C (1991) The stratigraphic signatures of tectonics, eustasy and sedimentology: an overview. In: Einsele G, Ricken W, Seilacher A (eds) Cycles and events in stratigraphy, 6th edn. Springer-Verlag, Berlin, pp 617–659
- Wada S (2008) Clays and soil pollution. *Nendokagaku (J Clay Sci Soc Jpn)* 47(3):185–195 (**in Japanese**)
- Wang N, Ouyang T, Yun SJ, Iwashima K (1997) The chemical forms of As in soils of Chiba prefecture. *Kankyo to Sokuteigijutu (Environ Meas Tech)* 24:7–11 (**in Japanese**)
- Williams LB, Hervig RL (2005) Lithium and boron isotopes in illite-smectite: the importance of crystal size. *Geochim Cosmochim Acta* 69:5705–5716
- Williams LB, Hervig RL, Holloway JR, Hutcheon I (2001) Boron isotope geochemistry during diagenesis: part 1. Experimental determination of fractionation during illitization of smectite. *Geochim Cosmochim Acta* 65:1769–1782
- Williams LB, Turner A, Hervig RL (2007) Intercrystalline boron isotope partitioning in illite-smectite: testing the geothermometer. *Am Miner* 92:1958–1965
- Yamaguchi H, Montani S (2002) Biological production in coastal seas with relation to benthic organisms. *Jpn J Limnol* 63:241–248 (**in Japanese with English abstract**)
- Yasuhara M, Irizuki T, Yoshikawa S, Nanayama F (2002) Holocene sea-level changes in Osaka Bay, western Japan: ostracode



evidence in a drilling core from the southern Osaka Plain. *J Geol Soc Jpn* 108(10):633–643

Yasutaka T, Imoto Y, Kurosawa A, Someya M, Higashino K, Kalbe U, Sakanakura H (2017) Effects of colloidal particles on the results and reproducibility of batch leaching tests for heavy metal-contaminated soil. *Soils Found* 57:861–871

Zimmerman AJ, Weindorf DC (2010) Heavy metal and trace metal analysis in soil by sequential extraction: a review of procedures. *Int J Anal Chem* 2010:1–7. <https://doi.org/10.1155/2010/387803>

**Publisher's Note** Springer Nature remains neutral with regard to jurisdictional claims in published maps and institutional affiliations.